

# Mutual Coupling Reduction in Multiband MIMO Antenna Using Cross-Slot Fractal Multiband EBG in the *E*-Plane

Niraj Kumar<sup>1,\*</sup>, Usha K. Kommuri<sup>1</sup>, and Priyanka Usha<sup>2</sup>

**Abstract**—A multiband electromagnetic band gap (EBG) structure is designed and implemented with a multiband MIMO antenna for mutual coupling reduction. An area of  $16 \times 16 \text{ mm}^2$  on a low cost FR4 substrate is used for the proposed EBG design. The designed E-coupled slotted U-shape MIMO antenna resonates at 5.7 GHz, 7.5 GHz, and 10 GHz frequencies. Edge to edge separation between the two antennas is kept as 6 mm. EBG structure is placed in the ground plane between two antennas that enable us to keep the separation of antennas less than the size of the EBG. Mutual coupling gets reduced by 6.6 dB for 5.7 GHz, 4 dB for 7.5 GHz, and 6.95 dB for 10 GHz. Simulated radiation properties of MIMO antenna are verified by measured results, and surface current distribution of MIMO antenna surface also verifies the mutual coupling reduction. Envelope correlation coefficient  $< 0.01$  and channel capacity loss  $< 0.2$  are achieved at resonating frequencies.

## 1. INTRODUCTION

Multiband multiple-input multiple-output (MIMO) antenna technology is an important aspect of modern wireless communications, as it helps to improve the performance and efficiency of wireless networks. This technology is used in many different applications, including cellular networks, Wi-Fi, and other wireless communication systems. In wireless communication services, multiband antenna systems are in high demand due to their transmission and reception at different frequency bands. To enhance the data transmission rate, MIMO antenna technology is used in multiband antenna. The space for placement of antenna is restricted due to increasing demand for compact devices. When multiple antennas are placed in a small space, the mutual coupling between the antenna elements dominates, and it affects the operation of an entire wireless system. The mutual coupling between these elements leads to the change in radiation properties and change in input matching circuits. Due to these problems, it is required to design a MIMO antenna system having low mutual coupling and compact size.

Many techniques have been mentioned in the literature for minimizing the multiband mutual coupling between the antenna elements. In [1], a novel decoupling structure, consisting of two inverted-L branches and a rectangular slot with one circular end, etched on the ground plane, was introduced to achieve low mutual coupling below 15 dB for all matched frequency bands. A dumb-bell shape parasitic element is inserted between the two circular patch antennas in [2] to reduce mutual coupling. In [3], the isolation is enhanced at the lower band by inserting a metal strip and at higher band by inserting a T shaped stub. [4] uses the orthogonal orientation of antennas to reduce the mutual coupling. One dipole is etched on the top of a two-layered dielectric substrate, and the other is printed on the bottom side of the same substrate. They are located orthogonal to one another. In [5], the first antenna at port 1 is fixed in its position and orientation while the orientation of second antenna element is changed in six different orientations and gives the least interference and insertion loss. Defected ground structure is

---

Received 31 January 2023, Accepted 27 March 2023, Scheduled 6 April 2023

\* Corresponding author: Niraj Kumar (nirajkumar@vit.ac.in).

<sup>1</sup> School of Electronics Engineering, Vellore Institute of Technology Chennai, India. <sup>2</sup> Department of Engineering Design, Indian Institute of Technology Madras, Chennai, India.

embedded between two trapezoidal-shaped patches in [6]. Complementary split-Ring resonator (CSRR) is used in [7]. A defect is introduced in the ground plane for minimizing the mutual coupling in [8].

Many other methods have been presented in the literature to get isolated MIMO antennas [9–16]. The majority of the previous works have utilized H-coupling to arrange the MIMO antenna elements. The coupling in  $E$ -plane is greater than the coupling in  $H$ -plane due to facing of radiating edges. Hence, a decoupling structure for mutual coupling reduction in  $E$ -plane for multiband is needed. EBG structures can effectively reduce the mutual coupling between multiple antennas in a MIMO system, which leads to improved signal quality and increased data throughput. By reducing mutual coupling, EBG structures can improve the performance of individual antennas in a MIMO system, allowing for better signal transmission and reception. It can also provide enhanced signal isolation between different frequency bands in a MIMO system, which helps to prevent interference and improve signal quality. EBG structures can help to simplify MIMO antenna systems and reduce their size, making them more practical and cost-effective. Electromagnetic band gap (EBG) structures are being used in MIMO antennas for mutual coupling reduction in both  $E$  and  $H$ -planes [17, 18].

This research work proposes the design of a multiband EBG structure and its application in  $E$ -plane coupled multiband MIMO antenna mutual coupling reduction. The edge to edge gap of MIMO antenna elements is minimized by using a half ground structure, and placing the EBG in the space is available in the ground plane.

## 2. DEVELOPMENT AND ANALYSIS OF UNIT CELL OF MULTIBAND ELECTROMAGNETIC BAND STRUCTURE

A novel multiband EBG structure is designed using multiple cross slots, surrounded by comb shape structures and four rectangular slots at the four corners. The proposed EBG acquires an area of  $16 \times 16 \text{ mm}^2$  on an FR4 substrate with the dielectric constant of 4.4 and thickness of 1.6 mm. The unit cell structure with detailed dimensions is shown in Fig. 1, and optimised parameters are shown in Table 1. Considering the available fabrication limitations, the minimum dimension is limited to 0.2 mm as shown in Table 1. The proposed unit cell structure is designed by cutting slots in a rectangular patch, and thus it is very easy to design with reduced design complexity.

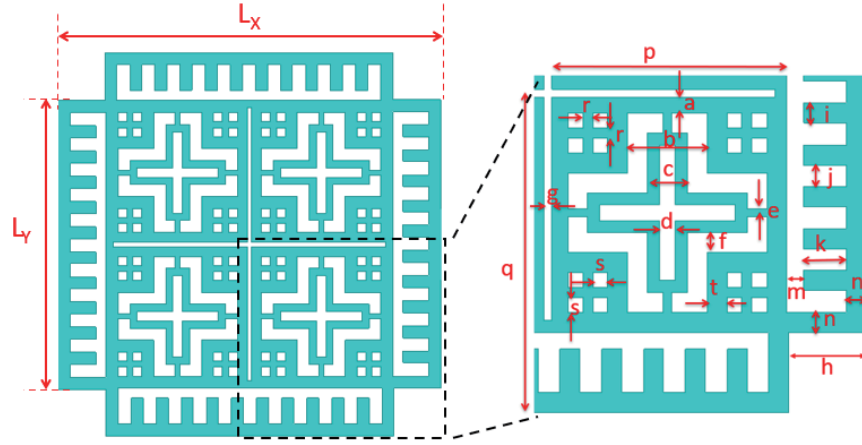


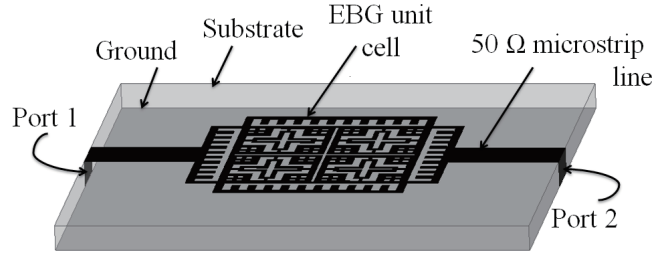
**Figure 1.** Unit cell of proposed EBG structure.

The proposed EBG is symmetrical in design, and the development of cross structures is based on the fractal geometry technique. At first, the proposed EBG unit cell is analyzed for the band gap using transmission line analysis method.

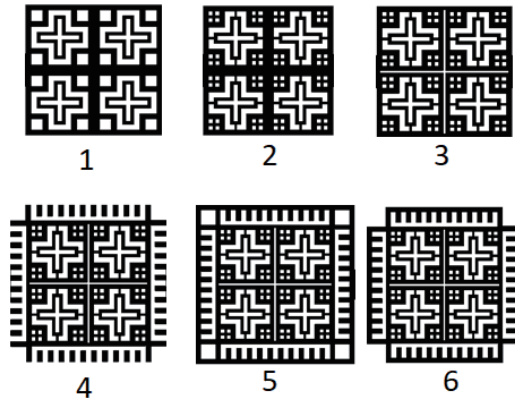
A  $50 \Omega$  transmission line with two ports is created on an FR4 substrate, and its transmission characteristics have been simulated with HFSS. Transmission characteristics of  $50 \Omega$  transmission line are compared with transmission characteristics of the transmission line with the proposed EBG placed in the center of the upper surface. Setup for the transmission line analysis is shown in Fig. 2.

**Table 1.** Optimized values of parameters of EBG unit cell.

Parameters	$L_X$	$L_Y$	$a$	$b$	$c$	$d$	$e$	$f$	$g$	$h$
values (mm)	16	12	0.4	2	1	0.4	0.2	0.5	0.2	2
Parameters	$i$	$j$	$k$	$m$	$n$	$p$	$q$	$r$	$s$	$t$
values (mm)	0.5	0.55	1.1	0.4	0.5	5.9	7.9	0.25	0.4	0.5

**Figure 2.** Unit cell transmission line analysis setup.

Different design stages of unit cell design and their transmission characteristics are shown in Figs. 3 and 4. In the first stage, we make four cross structures for the basic structure of unit cell and get reduced transmission coefficient at 13 GHz and 18 GHz. Sixteen smaller cross structures are created in the remaining available space in EBG basic structure in stage 2, and it gives reduced transmission coefficient at 12.5 GHz and 17.6 GHz. Etching out an extra cross slot at the midsection of EBG changes the frequency of interest to 8.5 GHz and 17 GHz. Finally, surrounding the cross structure with the comb shape structures and optimizing it in the fourth, fifth and sixth stages give reduced transmission coefficient for three center frequencies 5.9 GHz, 9.5 GHz, and 13.5 GHz.

**Figure 3.** Design stages of multiband EBG unit cell.

The proposed EBG gives multiple resonances due to its multiple resonating structures in a single unit cell in the form of different shapes of slots. This EBG contains mostly rectangular shape elements in the unit cell which leads to a sharper stopband. These properties can be used to stop the transmission of surface waves between elements of multiband MIMO antennas. By optimizing the values of different parameters of proposed EBG structure as shown in Fig. 1, band gaps of 5.6–6.6 GHz (C-band), 9–11.6 GHz (X-band), and 12.6–14.7 GHz (Ku-band) are achieved.

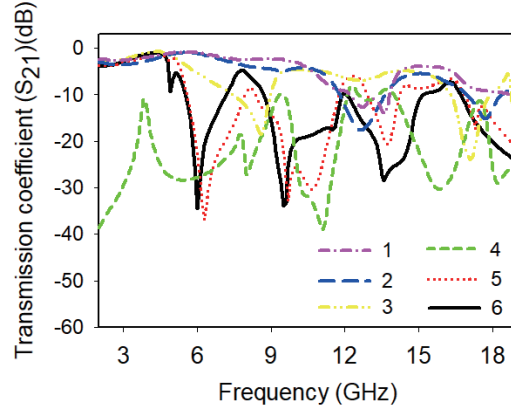


**Figure 4.** Transmission coefficient for all design stages.

### 3. DESIGN OF MULTIBAND MIMO ANTENNA AND APPLICATION OF EBG IN MULTIBAND MUTUAL COUPLING REDUCTION

One element of the MIMO antenna is designed as a triple band antenna on an FR4 substrate with a U-shape radiating patch with a slot in the radiating patch and modified ground structure. The proposed antenna is shown in Fig. 5, and optimised parameters are as shown in Table 2.

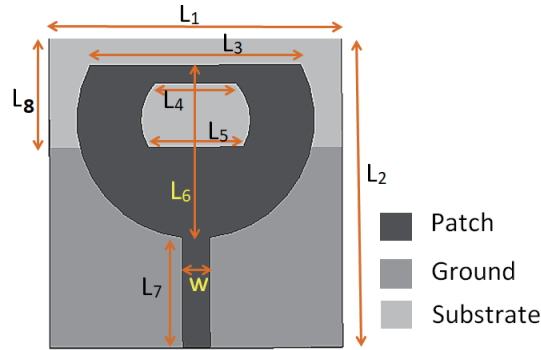


**Figure 5.** Multiband antenna design.

**Table 2.** Optimized values of parameters of multiband antenna.

Parameters	$L_1$	$L_2$	$L_3$	$L_4$	$L_5$	$L_6$	$L_7$	$L_8$	$W$
values (mm)	32	34	23	9	10.4	19	12	12	3

Only one element (slot) has been used for creating three bands. The slot in the patch has two parallel edges and two curved edges. The upper edge of the slot is parallel with edge of the ground just below it on the opposite side of the substrate. This multiband antenna resonates at frequencies 5.7 GHz, 7.5 GHz, and 10 GHz.

Two closely spaced elements of multiband antennas are arranged in  $E$ -plane as shown in Fig. 6(a). Reducing the edge-to-edge separation between MIMO antenna elements can result in stronger coupling between the antennas. This can lead to improved diversity gain, which is the ability of the MIMO system to maintain a stable signal quality even in the presence of fading or interference. However, strong coupling can also lead to an increase in mutual coupling, which can degrade the MIMO system's

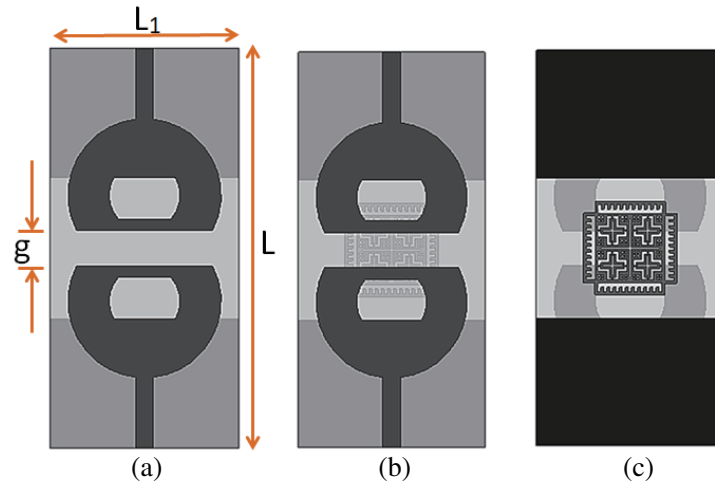


**Figure 6.** Multiband MIMO antenna design (a) without EBG (b) with EBG front view (c) with EBG back view ( $L_1 = 32$  mm,  $L = 68$  mm,  $g = 6$  mm).

performance by introducing interference between the antenna elements. Hence, edge to edge gap ‘ $g$ ’ is optimized to 6 mm to achieve compactness along with antenna performance, and the proposed EBG is inserted in the ground plane at the center as shown in Figs. 6(b) and (c).

Half ground of the antenna elements gives the opportunity to place the EBG in ground plane between the antenna elements. This way, the large size of EBG unit cell does not increase the edge to edge distance of the antennas due to implementation in the ground plane and helps in reducing the mutual coupling in top plane as well as the ground plane. It helps in achieving the compactness of MIMO antenna and reducing the mutual coupling simultaneously.

The proposed MIMO antennas with EBG and without EBG are fabricated on an FR4 substrate by photo-lithography process. Fabricated multiband MIMO antenna front views and back views without and with EBG are shown in Fig. 7. Measurement of the antenna parameters has been done in an anechoic chamber using vector network analyzer (VNA).

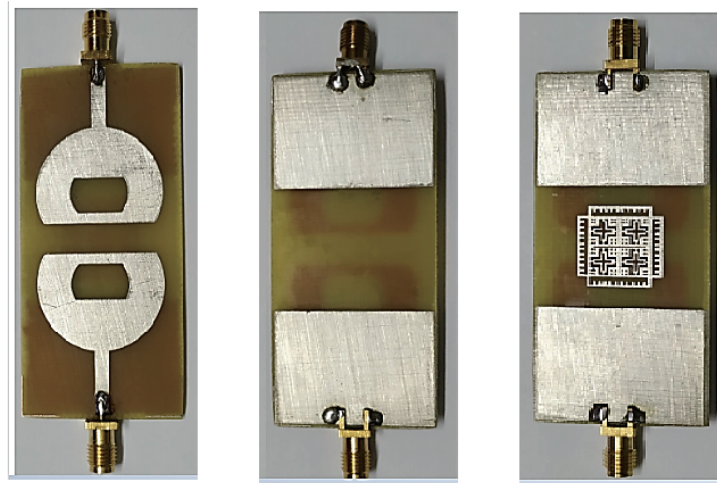


**Figure 7.** Fabricated multiband MIMO antenna front view and back view without and with EBG.

#### 4. RESULTS AND DISCUSSION

Figure 8 shows the simulated and measured return losses ( $S_{11}$ ) of a  $2 \times 1$  MIMO antenna. The simulated results without EBG gives three frequency bands 5.46–6.09 GHz, 7.20–7.96 GHz, and 9.58–10.72 GHz with center frequencies 5.77 GHz, 7.58 GHz, and 10.15 GHz, respectively. On the other hand, after the implementation of EBG the frequency bands are 5.43–6.04 GHz, 7.35–7.93 GHz, and 9.46–10.98 GHz with center frequencies 5.73 GHz, 7.64 GHz, and 10.22 GHz, respectively. It is noticed that there is a slight shift of frequencies after implementing the EBG structure. The measured results without EBG give three frequency bands 5.73–6.16 GHz, 7.45–7.99 GHz, and 9.45–11.6 GHz with center frequencies 5.94 GHz, 7.72 GHz, and 10.52 GHz, respectively. After the implementation of EBG, measured frequency bands are 5.58–6.15 GHz, 7.5–8.05 GHz, and 9.56–12.6 GHz with center frequencies 5.86 GHz, 7.77 GHz, and 11.08 GHz, respectively. It can be observed that the simulated and measured return losses are in good match for both the cases, i.e., without and with EBG.

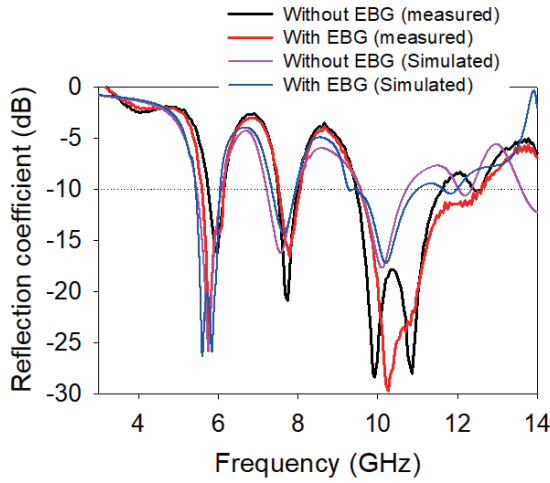


**Figure 8.** Simulated and measured return losses with and without EBG.

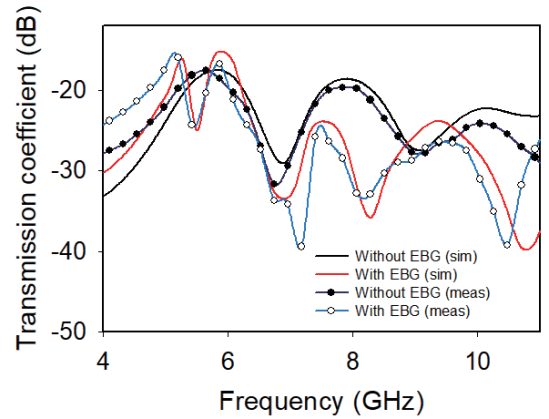


**Figure 9.** Simulated and measured mutual couplings with and without EBG.

The simulated and measured transmission coefficients between the MIMO antenna elements are compared in Fig. 9. It shows that after applying the EBG structure simulated mutual coupling is reduced for the frequency bands 5.38–5.73 GHz, 6.22–8.88 GHz, and 9.56–11.8 GHz with maximum reduction at 5.53 GHz, 6.9 GHz, and 10.77, respectively.

The simulated mutual coupling is reduced from  $-18.22$  dB to  $-24.9$  dB at 5.7 GHz,  $-19.86$  dB to  $-23.82$  dB at 7.5 GHz, and  $-22.1$  dB to  $-28.45$  dB at 10 GHz. After applying the EBG, measured mutual coupling is also reduced for the frequency bands 5.27–5.74 GHz, 5.94–9.04 GHz, and 9.5–10.86 GHz with maximum reduction at 5.48 GHz, 7.16 GHz, and 10.48 GHz, respectively. The measured mutual coupling is reduced from  $-17.7$  dB to  $-24.3$  dB at 5.7 GHz,  $-20.7$  dB to  $-24.7$  dB at 7.5 GHz, and  $-24.1$  dB to  $-31.05$  dB at 10 GHz. According to the results, the simulated mutual coupling is reduced by 6.68 dB at 5.7 GHz, 3.96 dB at 7.5 GHz, and 6.35 dB at 10 GHz, while the measured mutual coupling is reduced by 6.6 dB at 5.7 GHz, 4 dB at 7.5 GHz, and 6.95 dB at 10 GHz. This suggests that the EBG structure is effective in reducing mutual coupling at different frequencies, as predicted by the simulations and verified through experimental measurements. Moreover, measured results suggest that a minimum isolation of 24.3 dB is achieved for all three resonance frequency bands after implementing EBG structure. This means that the isolation between the antenna elements is strong enough to mitigate the interference and maintain a high signal quality in the MIMO system. Overall, these results demonstrate the effectiveness of using an EBG structure to reduce mutual coupling and improve the performance of MIMO antennas in different frequency bands.

Figure 10 shows the surface current density in the upper elements of antenna by providing feed from the lower elements. It is observed that the surface current density without EBG is higher than that

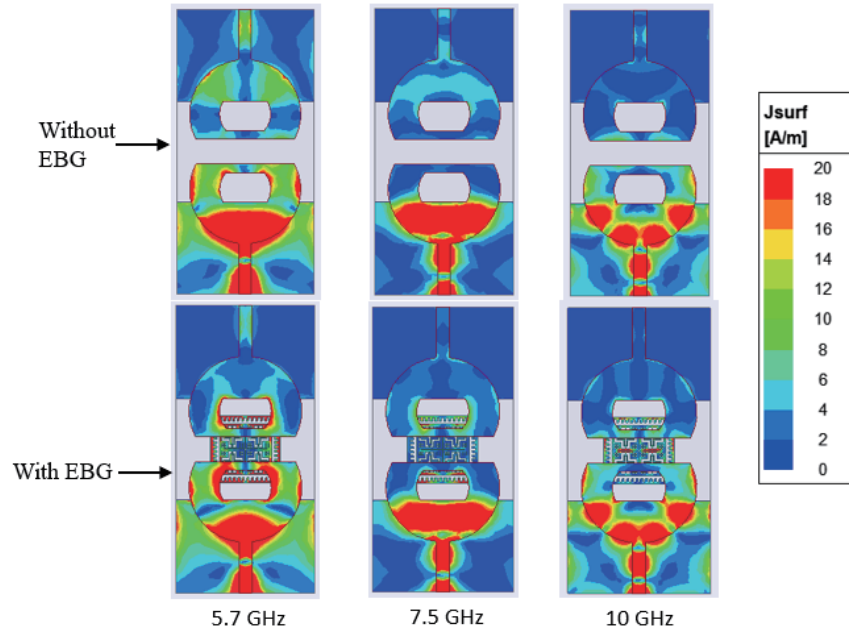


**Figure 10.** Surface current distribution of MIMO antenna with and without EBG at 5.7 GHz, 7.5 GHz and 10 GHz.

with EBG for all the resonant frequencies 5.7 GHz, 7.5 GHz, and 10 GHz. This indicates that there is a higher flow of current between the antenna elements without EBG, which leads to a stronger coupling and higher mutual coupling between the elements. On the other hand, the surface current density in the coupled antenna with EBG is lower, which implies that the mutual coupling is reduced with the EBG. The EBG structure acts as a filter, suppressing the coupling between the antenna elements and reducing the surface current density. This is consistent with the previously described results of reduced mutual coupling with the EBG. The comparison of the surface current distribution for the MIMO antenna with and without EBG provides additional evidence that the EBG structure is effective in reducing mutual coupling between antenna elements. This is important for improving the performance and signal quality of MIMO systems, especially in wireless communication applications.

Radiation patterns with and without EBG are plotted for all the three resonant frequencies 5.7 GHz, 7.5 GHz, and 10 GHz as shown in Fig. 11. It is observed from the comparison of plots of total  $E$ -field in  $E$ - and  $H$ -planes that the radiation patterns of antenna without EBG are not affected by EBG insertion for all the resonant frequencies.

A MIMO antenna system isolation can be verified with envelope correlation coefficient ( $\rho_e$ ) and channel capacity loss (CCL) values. To calculate the envelope correlation coefficient (ECC), two different approaches are used, first using far-field radiation pattern and second using scattering parameters. The scattering parameters method is preferred over far field radiation pattern method due to its ease of calculation. The envelope correlation coefficient of a two antennas system is determined using Eq. (1)

$$\rho_e = \frac{|S_{11}^* S_{12} + S_{21}^* S_{22}|^2}{(1 - |S_{11}|^2 - |S_{21}|^2)(1 - |S_{22}|^2 - |S_{12}|^2)} \quad (1)$$

The channel capacity loss ( $C_{loss}$ ) can be calculated using Eq. (2).

$$C_{loss} = -\log_2 \det(\psi_R) \quad (2)$$

where  $\psi_R$  represents the correlation matrix of receiving antenna, and it is calculated using Eq. (3).

$$\psi_R = \begin{bmatrix} (1 - |S_{11}|^2 - |S_{21}|^2) & -(S_{11}^* S_{12} + S_{21}^* S_{22}) \\ -(S_{22}^* S_{21} + S_{12}^* S_{11}) & (1 - |S_{22}|^2 - |S_{12}|^2) \end{bmatrix} \quad (3)$$



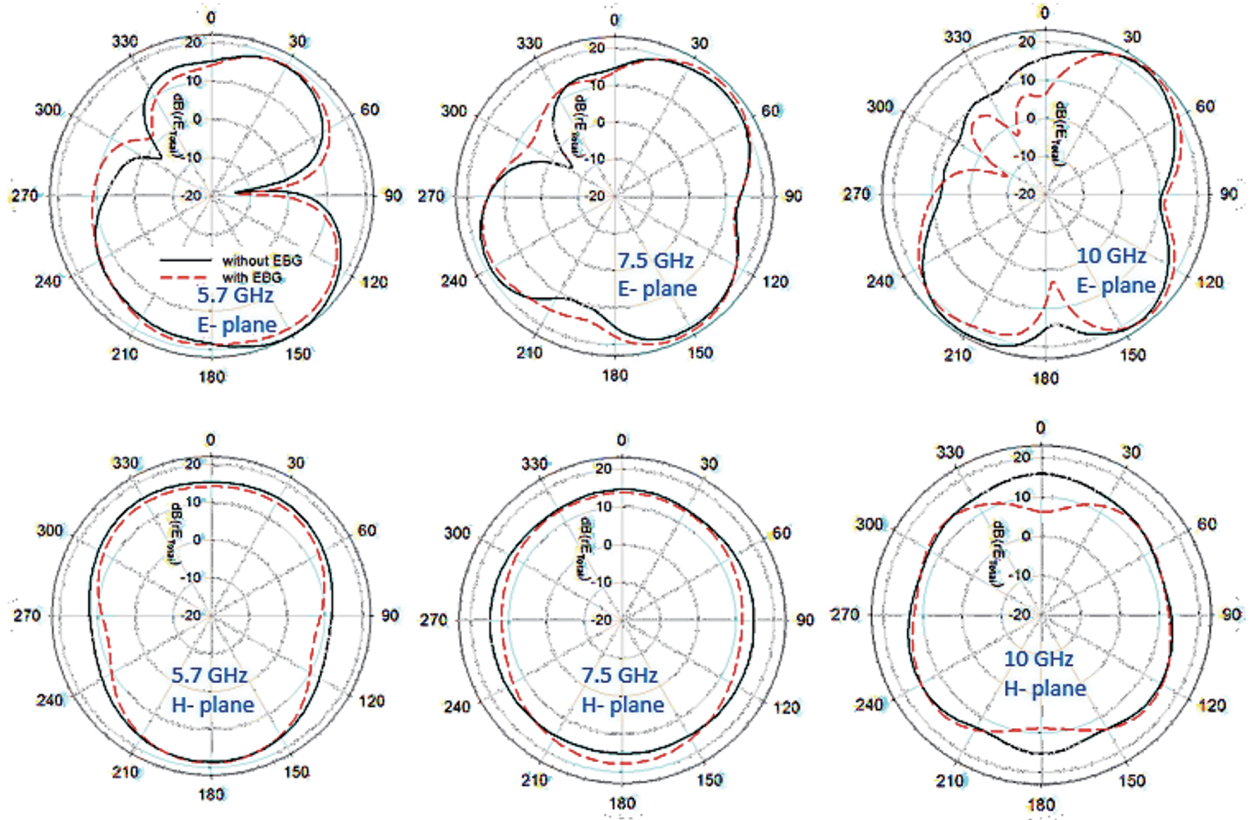


**Figure 11.** *E*-plane (top) and *H*-plane (bottom) radiation pattern of MIMO antenna with and without EBG at 5.7 GHz, 7.5 GHz and 10 GHz.

For a multi-antenna system to be isolated, both the parameters ECC ( $\rho_e$ ) and CCL ( $C_{loss}$ ) should have low values at resonant frequencies. Fig. 12 shows that the simulated ECC values without EBG are  $1.37 \times 10^{-4}$  at 5.7 GHz,  $1.68 \times 10^{-4}$  at 7.5 GHz, and  $2.97 \times 10^{-5}$  at 10 GHz. After applying EBG, ECC values are  $1.029 \times 10^{-4}$  at 5.7 GHz,  $1.99 \times 10^{-4}$  at 7.5 GHz, and  $1.96 \times 10^{-5}$  at 10 GHz. These values of ECC are well within the permissible value ( $ECC < 0.01$ ). Fig. 13 shows that the CCL is 0.065

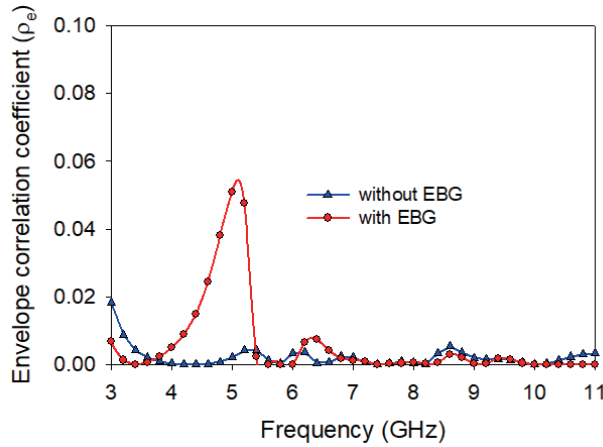


**Figure 12.** Envelope correlation coefficient of MIMO antenna with and without EBG.

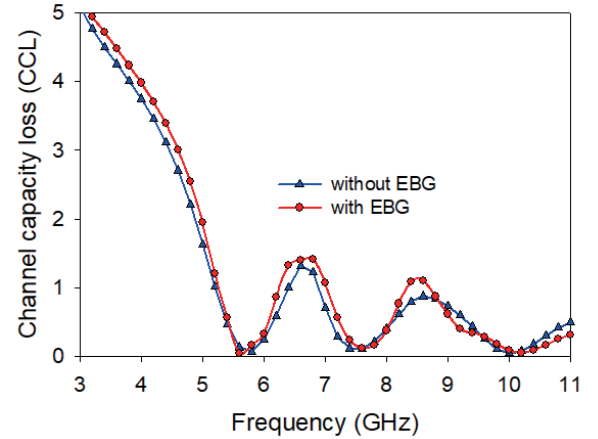


**Figure 13.** Channel capacity loss of MIMO antenna with and without EBG.



at 5.7 GHz, 0.096 at 7.5 GHz, and 0.04 at 10 GHz without applying EBG. The CCL values are 0.083 at 5.7 GHz, 0.15 at 7.5 GHz, and 0.08 at 10 GHz after implementing the EBG structure. These values are also within the required limit ( $CCL < 0.2$ ).

Table 3 shows the comparison of existing works related to multiband MIMO antenna isolation with the proposed works. In [1], a multiband antenna for 5 bands is presented with  $H$ -plane coupling and a reduced edge to edge gap of  $0.0972\lambda_0$ , but the physical dimension of edge to edge gap is 32.4 mm which is quite large due to the presence of a lower frequency. Moreover, the minimum isolation is only 15 dB. In [2], the minimum isolation is 30 dB, but the edge to edge gap is 20 mm physically and  $0.233\lambda_0$  electrically. In [3], the physical dimension of edge to edge gap is 17.6 mm; electrical dimension is  $0.141\lambda_0$ ; and the minimum isolation is 20 dB. [4] presents a different technique for mutual coupling reduction by placing the antenna elements orthogonally, and the structure becomes very compact, but it leads to polarization diversity. In [7], the edge to edge gap is less, but it has only explored the lower frequencies. Overall, the proposed design is compact and coupled in  $E$ -plane with the minimum isolation of 24.3 dB with less physical as well as electrical dimension of edge to edge gap between the elements.

**Table 3.** Comparison of proposed work with existing works.

Ref No.	Edge to edge gap (mm)/in terms of free space wavelength ( $\lambda_0$ ) of the lowest frequency	Material used ( $\epsilon_r$ )	type of coupling	No. of bands	Freq. (GHz)	Min isolation (dB)
[1]	32.4/ $0.0972\lambda_0$	4.4	$H$ -plane	5	0.9, 1.800, 2.1, 3.5, 5.4	15
[2]	20/ $0.233\lambda_0$	4.4	$H$ -plane	3	3.5, 5.5, 7.5	30
[3]	17.6/ $0.141\lambda_0$	4.4	$H$ -plane	3	2.4, 5.2, 5.8	20
[4]	0.8/ $0.002\lambda_0$	4.4	orthogonal	2	0.75, 2.5	20
[7]	12/ $0.035\lambda_0$	4.3	orthogonal	3	0.875, 1.8, 2.45	10
<b>This work</b>	6/ $0.11\lambda_0$	4.4	$E$ -plane	3	5.7, 7.5, 10	24.3

## 5. CONCLUSION

This work presents the isolation enhancement of a multiband MIMO antenna using a multiband EBG structure in  $E$ -plane. Fractal geometry consisting of rectangular slots is used for designing the proposed EBG. The different designing stages of EBG structure are analyzed using transmission line analysis and discussed. The transmission coefficient of the design in each stage is compared with the transmission coefficient of  $50\Omega$  line to get the band gap of the EBG structure. Multiband EBG is achieved by optimizing the size and position of rectangular slots of fractal geometry. The proposed multiband EBG structure is placed at the center of the ground plane of multiband MIMO antenna designed on a low cost FR4 substrate. Half ground of individual antennas and insertion of EBG in ground plane help in reducing the gap between radiating patches of the MIMO antenna elements. The isolation improvement for multiple bands is achieved for reduced edge to edge distance between the antenna elements. All the structures are simulated with ANSYS HFSS. Simulated results are verified with measured ones which are in a good match.

## REFERENCES

1. Shoaib, S., I. Shoaib, N. Shoaib, X. Chen, and C. G. Parini, "Design and performance study of a dual-element multiband printed monopole antenna array for MIMO terminals," *IEEE Antennas and Wireless Propagation Letters*, Vol. 13, 329–332, 2014.

2. Babu, K. V. and B. Anuradha, "Analysis of multi-band circle MIMO antenna design for C-band applications," *Progress In Electromagnetics Research C*, Vol. 91, 185–196, 2019.
3. Luo, C.-M., J.-S. Hong, and M. Amin, "Mutual coupling reduction for dual-band MIMO antenna with simple structure," *Radioengineering*, Vol. 26, No. 1, 51–56, 2017.
4. Han, M. and J. Choi, "Multiband MIMO antenna using orthogonally polarized dipole elements for mobile communications," *Microwave and Optical Technology Letters*, Vol. 53, No. 9, 2043–2048, 2011.
5. Aw, M., K. Ashwath, T. Ali, et al., "A compact two element MIMO antenna with improved isolation for wireless applications," *Journal of Instrumentation*, Vol. 14, No. 6, P06014, 2019.
6. Pouyanfar, N., C. Ghobadi, J. Nourinia, K. Pedram, and M. Majidzadeh, "A compact multi-band MIMO antenna with high isolation for C and X bands using defected ground structure," *Radioengineering*, Vol. 27, No. 3, 686–693, 2018.
7. Kumar, A., A. Q. Ansari, B. K. Kanaujia, and J. Kishor, "High isolation compact four-port MIMO antenna loaded with CSRR for multiband applications," *Frequenz*, Vol. 72, No. 9–10, 415–427, 2018.
8. Rao, P. S., K. J. Babu, and A. M. Prasad, "Compact multi-band MIMO antenna with improved isolation," *Progress In Electromagnetics Research M*, Vol. 62, 199–210, 2017.
9. Kumar, N. and K. U. Kiran, "Meander-line electromagnetic bandgap structure for uwb MIMO antenna mutual coupling reduction in  $E$ -plane," *AEU-International Journal of Electronics and Communications*, Vol. 127, 153423, 2020.
10. Wani, J., P. Camacho, R. S. Malfajani, and M. S. Sharawi, "Design and fabrication of a multi-band 2 element MIMO antenna for sub-6 GHz applications," *2021 IEEE Indian Conference on Antennas and Propagation (InCAP)*, 198–200, 2021.
11. Shiddanagouda, F., N. Kumar, R. Vani, and P. Hunagund, "Two element multi-band MIMO antenna for WIFI/5G/WLAN band applications," *2021 IEEE Microwave Theory and Techniques in Wireless Communications (MTTW)*, 102–106, 2021.
12. Saleem, R., M. Bilal, H. T. Chattha, S. Ur Rehman, A. Mushtaq, and M. F. Shafique, "An FSS based multiband MIMO system incorporating 3d antennas for WLAN/WIMAX/5G cellular and 5G WI-FI applications," *IEEE Access*, Vol. 7, 144732–144740, 2019.
13. Das, G., A. Sharma, R. K. Gangwar, and M. S. Sharawi, "Performance improvement of multiband MIMO dielectric resonator antenna system with a partially reflecting surface," *IEEE Antennas and Wireless Propagation Letters*, Vol. 18, No. 10, 2105–2109, 2019.
14. Zhang, B., J. M. Jornet, I. F. Akyildiz, and Z. P. Wu, "Mutual coupling reduction for ultra-dense multi-band plasmonic nano-antenna arrays using graphene-based frequency selective surface," *IEEE Access*, Vol. 7, 33214–33225, 2019.
15. Zhao, X. and S. Riaz, "A dual-band frequency reconfigurable MIMO patch-slot antenna based on reconfigurable microstrip feedline," *IEEE Access*, Vol. 6, 41450–41457, 2018.
16. Jaglan, N., S. D. Gupta, B. K. Kanaujia, and M. S. Sharawi, "10 element sub-6-GHz multi-band double-T based MIMO antenna system for 5G smartphones," *IEEE Access*, Vol. 9, 18662–18672, 2021.
17. Kumar, N. and U. K. Kommuri, "MIMO antenna mutual coupling reduction for wlan using spiro meander line UC-EBG," *Progress In Electromagnetics Research C*, Vol. 80, 65–77, 2018.
18. Kumar, N. and U. K. Kommuri, "MIMO antenna  $H$ -plane isolation enhancement using UC-EBG structure and metal line strip for WLAN applications," *Radio Engineering*, Vol. 29, No. 2, 399–406, 2019.